Organic & Biomolecular Chemistry

Accepted Manuscript

This article can be cited before page numbers have been issued, to do this please use: F. Wu, M. Yang, J. Deng, D. Guo, J. Zhang and L. X. Yang, *Org. Biomol. Chem.*, 2019, DOI: 10.1039/C9OB00698B.

ROYAL SOCIETY OF CHEMISTRY

rsc.li/obc

View Article Online
DOI: 10.1039/C9OB00698B

Folate-Conjugated Platinum Porphyrin Complex as a New Cancer-Targeting Photosenitizer for Photodynamic Therapy

Mengqian Yang[a], Jingran Deng[a], Ding Guo[a], Jie Zhang[b]*, Lixia Yang[a], Fengshou Wu[a]*

[a] *Key Laboratory for Green Chemical Process of the Ministry of Education, School of Chemical Engineering and Pharmacy, Wuhan Institute of Technology, Wuhan, 430205, P. R. China. Email: wfs42@126.com; fswu@wit.edu.cn.*

[b] *Department of Chemistry, School of Pharmaceutical and Chemical Engineering, Taizhou University, Taizhou, 318000, P. R. China. Email: zhang_jie@tzc.edu.cn.*

Abstract

A new folate-conjugated platinum porphyrin complex (Por 4) was synthesized and characterized. The singlet oxygen production of the conjugates was evaluated through 1,3-diphenylisobenzofuran method. The targeting ability and subcellular localization of Por 4 were confirmed by confocal laser scanning microscope in HeLa cells (overexpression of FR) as well as A549 cells (low expression of FR). The results suggested that the modification of the carboxyl group with porphyrin compound did not decrease the binding affinity of folic acid with FR positive cancer cells. Moreover, the MTT assay using HeLa cells and A549 cells verified the low cytotoxicity of Por 4 in the dark. Upon irradiation, Por 4 showed noticeable improvement in toxicity against cancer cells with overexpression of FR. Upon the treatment of Por 4 at the concentration of 20 μM, the cell viability was determined as 22% and 75% for HeLa and A549 cells, respectively, indicating that the folate-conjugated platinum porphyrin complex could be a promising PDT agent for cancer with overexpresion of folate receptor.

Keywords: Porphyrin; targeting; photosensitizers; folic acid; PDT

1. Introduction

Cancer is one of the deadliest diseases threatening the human beings' health around the world. Among the emerging cancer therapy methods, photodynamic therapy (PDT) has gained considerable attentions because it is noninvasive in nature, has fewer side effects, and causes

negligible drug resistance.[1] The therapeutic mechanism of PDT is that the photosensitizer can generate reactive oxygen species (ROS), such as singlet oxygen ($^1O_2$) under the irradiation of specific wavelength light, which will effectively damage the structure and function of cancer cells.[2-4] Porphyrin and its derivatives have been widely studied as the efficient photosensitizers in photodynamic therapy (PDT). Some of them have been approved by the multinational governments drug regulatory authorities and were widely applied in clinic due to their strong photosensitizing effect, low toxicity and low side effects to the human body.[5,6] However, it is still confronted with several challenges, such as low biocompatibility and singlet oxygen yield and inadequate selectivity toward cancer tissues.[7] Accordingly, a PDT agent with good selectivity and high $^1O_2$ quantum yield is highly desirable.[8]

To enhance the therapeutic efficiency of photosensitizers and avoid the severe side effects on healthy tissues, the targeting delivery of anticancer drugs to tumor sites in a passive or active manner, is an effective method. Although passive targeting approaches provide a significant basis for clinical therapeutic treatments, they still suffer from several drawbacks, such as prolonged photosensitivity and photoalergic reactions.[9] In contrast, active targeting involves the attachment of targeting ligands to photosensitizer that can specifically recognize receptors overexpressed on the membrane of tumor cells. The targeting ligands, including monoclonal antibodies (anti-HER2, anti-EGFR[9,10]), small biomolecules (biotin[11]), peptides (TAT peptide[12] and RGD peptide[13]), and oligonucleotides (aptamers[14,15]) were widely reported in previous literatures. Folic acid (FA) is also a targeting agent which has been widely studied in the field of imaging or diagnostics [16-18] and for the treatment of certain cancers. Numerous cancer cell lines, such as prostate, brain, lung, nose, ovary, colon cancer [16,17] over-express FA receptors (FRs) because of their fast growth and cell division.[19] On the contrary, the folate receptors (FRs) have very low expression on normal cells.[20] Therefore, the anti-cancer drugs conjugated with FA can selectively accumulate in tumor tissue.[21,22]

On the other hand, $^1O_2$ is generated by energy transfer between the triplet excited state of photosensitizers and the ground state of O_2.[23-25] Thus, the introduction of heavy metal ions into porphyrins could enhance the probability of intersystem crossing, which in turn improves their capacity of singlet oxygen generation.[26,27] In our previous studies, we synthesized a series of metal porphyrin complexes and investigated the metal effect of porphyrins on their $^1O_2$ quantum

yield. Among the various metal porphyrin complexes, the platinated porphyrin showed the highest therapeutic activity compared to free base porphyrin and other metal porphyrin complexes, probably due to its high efficiency of $^1O_2$ generation.[28] In this context, here we designed and synthesized a new platinum porphyrin-folate conjugate as an efficient photosensitizer for tumor-targeting PDT. Specifically, nine methoxyl groups were introduced into the porphyrin component to improve the biocompatibility of PDT agent.[29] And the platinum is coordinated with porphyrin conjugate to enhance the photodynamic therapeutic effect of agent by the heavy atom effect. Moreover, a targeting molecule (folic acid) is bonded to the platinum porphyrin complex to enhance the tumor-targeting of the photosensitizer. As expected, the folate-conjugated platinum porphyrin complex (Por 4) displayed the high singlet oxygen quantum yield and strong targeting ability. The cytotoxicity and subcellular localization of Por 4 in cancer cells were further evaluated through MTT method and confocal laser scanning microscope, respectively.

Results and Discussion

Synthesis

The synthetic routes of folic acid-platinum porphyrin conjugate (Por 4) were demonstrated in Scheme 1. Firstly, Por 1 was synthesized by condensation of pyrrole with 3,4,5-tri methoxybenzaldehyde and 4-formylbenzoic acid (3:1) in a refluxing of propionic acid. The Por 1 was then coordinated with potassium tetrachloroplatinate to obtain platinum porphyrin complex (Por 2). The activation of the carboxylic acid group was performed with thionyl chloride in dry pyridine, yielding the corresponding porphyrinic acyl chloride (Por 3). Due to the poor solubility of FA, its direct addition to the porphyrinic acyl chloride solution did not afford the desired product. Further addition of N-hydroxysuccinimide (NHS) at 50 °C afforded the activated ester Por 3 (Scheme 1). Finally, in the presence of N,N-diisopropylethylamine (DIEA), the carboxyl-activated folic acid was linked to the carboxyl-activated ester platinum porphyrin by ethylenediamine to synthesize a folic acid-platinum porphyrin conjugate (Por 4).

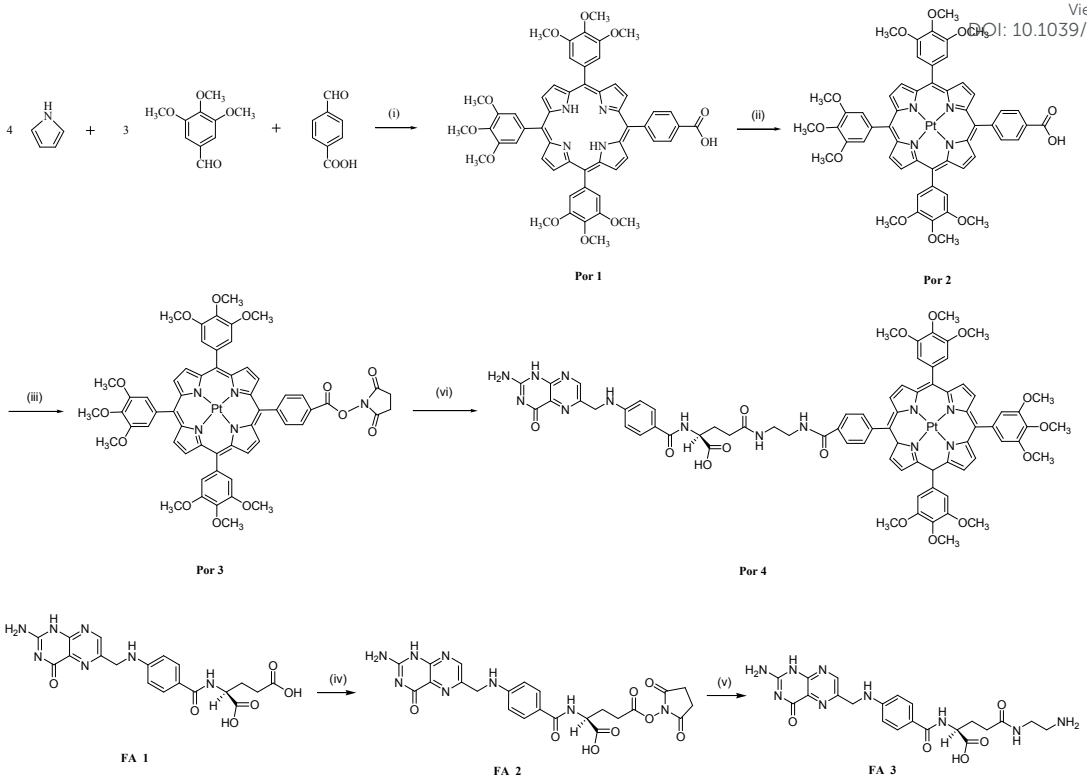

(i) acetic anhydride, propionic acid, 130 °C, 1.5 h, yield 6%; (ii) K_2PtCl_4, benzonitrile, 110 °C, 24 h, yield 78%; (iii) $SOCl_2$, NHS, pyridine, 50 °C, 3 h, yield 73%; (iv) DCC, NHS, DMSO, N_2, 6 h (v) Ethylenediamine, pyridine, rt, 12 h, yield 60%; (vi) FA 3, DIEA , DMF, N_2, 24 h, yield 34%.

Scheme 1. Synthetic routes of Por 1, Por 2, Por 3, FA 2, FA 3, and Por 4.

Photophysical properties

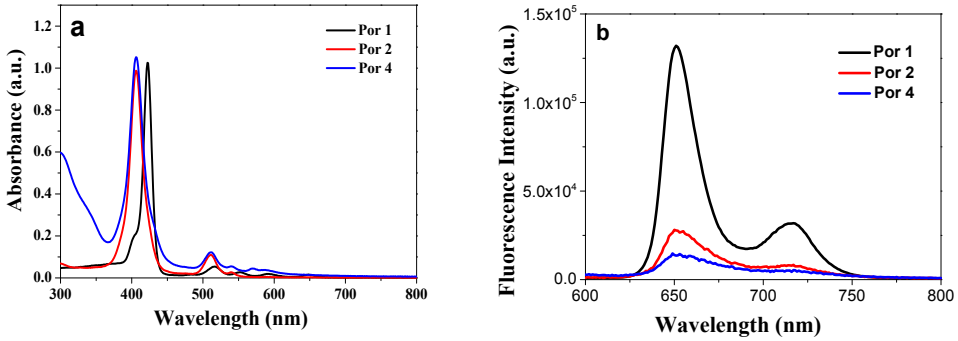

Fig. 1. (a) UV-vis absorption spectrum, and (b) emission spectrum of the intermediates and targeted compound.

Since Por 3 was not very stable, its photophysical properties were not recorded and investigated. The photophysical properties of Por 1, Por 2 and Por 4 were studied in DMF solution. The UV-vis absorption spectrum of Por 1 (Fig. 1a) exhibited a sharp Soret band centered at 422 nm and weak

Q bands at 516, 552, 591 and 648 nm, respectively. The two peaks in the Q bands of Por 2 and Por 4 disappeared, probably due to the metallization of porphyrin. Meanwhile, the Soret band of porphyrin showed a certain hypsochromic shift after coordination with metal. As shown in Fig. 1a, the Soret band of Por 1 was located at 422 nm, while Por 2 and Por 4 shifted to 406 nm, ascribed to the strong d_{π}-$e_g(\pi^*)$ π-dative interaction between Pt ion and porphyrin macrocycle.[30] The fluorescence emission of Por 1, Por 2 and Por 4 was tested in DMF solution. As shown in Fig. 1b, both of platinum porphyrin complexes (Por 2 and Por 4) exhibited red emission (λ_{em}= 650, 740 nm) with fluorescence intensity lower than that of free base porphyrin (Por 1), probably due to the heavy metal effect. The fluorescence quantum yields of Por 2 and Por 4 were determined to be 0.34 and 0.23, respectively. These results suggested that the conjugation of folic acid did not affect the wavelength of emission peaks.

Singlet oxygen detection

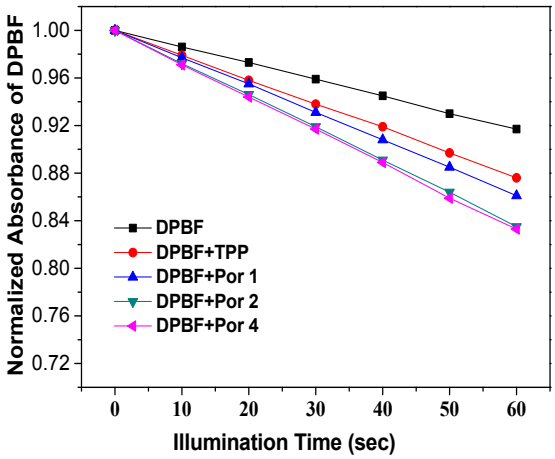

Fig. 2 The changes of absorbance at the characteristic peak of DPBF (418 nm) as a function of irradiation time.

The singlet oxygen ($^1O_2$) generation ability of Por 1, Por 2 and Por 4 was studied with the singlet-oxygen trap molecule 1,3-diphenylisobenzofuran (DPBF). DPBF is a good singlet oxygen scavenger, which was widely used in the measurement of $^1O_2$. The relative consumption of the capture agent, that is, the degree of attenuation of the absorbance, reflects the generation efficiency of singlet oxygen. As shown in Fig. 2, the absorbance of DPBF displayed a time-dependent decrease in reaction with singlet oxygen, generated from

porphyrins when irradiated with a LED lamp. Using tetraphenylporphyrin (TPP) as a reference, the singlet oxygen quantum yield of Por 1, Por 2, and Por 4 was calculated to be 0.72, 0.85 and 0.88, respectively. Under the same condition, the absorbance intensity of DPBF that mixed with Por 1 decreased more compared with that of tetraphenylporphyrin after irradiation for 60 s, suggesting the methoxyporphyrin had the higher singlet oxygen quantum yield, probably due to the better biocompatibility. In addition, since the capacity of photosensitizer to generate $^1O_2$ is dependent on the efficiency of the intersystem crossing (ISC) from ^{1}PS* to ^{3}PS*, the platinated porphyrins (Por 2 and Por 4) showed higher singlet oxygen quantum yield related to that of Por 1, due to the heavy-atom effect of metal platinum.

FR-mediated targeting for HeLa Cells

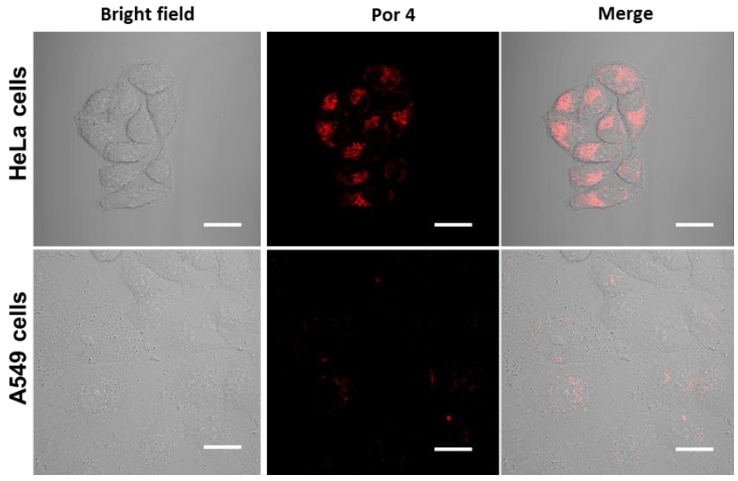

Fig. 3 Laser scanning confocal microscopy images (excited at 488 nm laser) of HeLa and A549 cells incubated with Por 4 at a concentration of 2.0 μM in the cell culture medium at 37 °C for 4 h. (The scale bar is 20 μm)

Next, we evaluated the targeting ability of Por 4, where the sample was incubated with FR-positive cell lines (HeLa cells) and FR-negative cell lines (A549 cells) at 2.0 μM, respectively, and then analyzed by confocal fluorescence imaging. As shown in Fig. 3, the HeLa cells (the first row of Fig. 3) displayed strong red fluorescent signals after 4 h of incubation with Por 4. In contrast, very weak red fluorescent signals were observed in A549 cells (the second row of Fig. 3) under the same condition, indicating that Por 4 could target specifically the cancer cells with overexpression of FR via FR-mediated endocytosis.

Subcellular localization

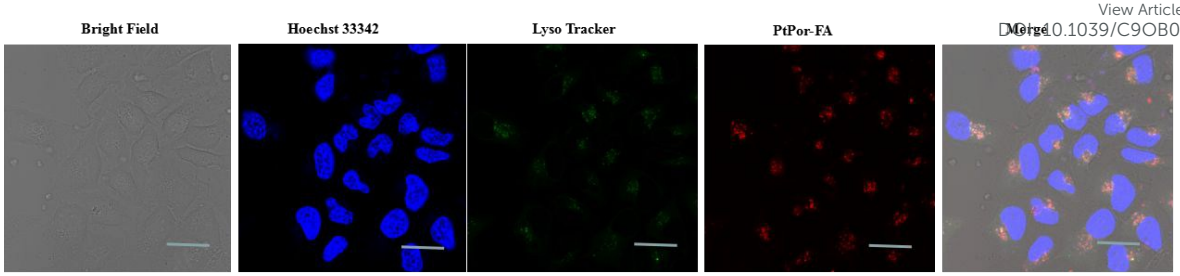

Fig. 4 Laser scanning confocal microscopy images (excited at 488 nm laser) of HeLa cells incubated with Por 4 for 4 h. Lysosomes (green) were stained with LysoTracker Green (50 μM). The nucleus (blue) was stained with Hoechst 33342 (1 μg/mL). (The scale bar is 20 μm).

To further figure out the subcellular localization of Por 4 in HeLa cells, LysoTracker Green and Hoechst staining was applied to visualize cell lysosomes (green) and nucleus (blue), respectively. As shown in Fig. 4, the red emission from Por 4 is almost overlapped with that of green fluorescence of LysoTracker Green, demonstrated the conjugate mainly entered the lysosomes of cancer cells, probably ascribed to the endocytosis mediated by folate receptor.

In vitro dark cytotoxicity and photocytotoxicity

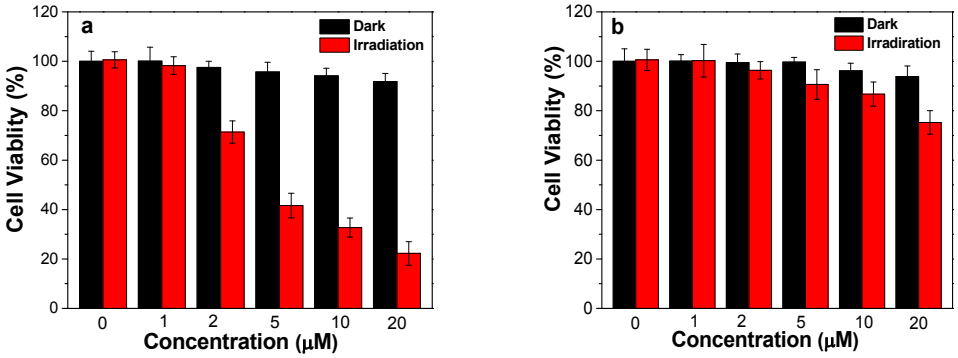

Fig. 5 HeLa (a), and A549 (b) cells viability at different concentrations (0, 1, 2, 5, 10, and 20 μM) of Por 4 for 4 h at 37 °C without or with irradiation for 30 min.

HeLa and A549 cells were utilized to evaluate the in vitro cytotoxicity of Por 4 via MTT assays. As shown in Fig. 5, Por 4 exhibited minor cytotoxicity toward HeLa and A549 cells in the dark with the increase of Por 4 from 0 to 20 μM. The surviving fractions of two cancer cells was both over 90% with the incubation of 20 μM Por 4, demonstrating that Por 4 had favorable biocompatibility with cells in all testing concentrations. Meanwhile, the photocytotoxicity of the synthesized porphyrin was also evaluated by a similar protocol. Obviously, Por 4 showed the significantly therapeutic efficacy against HeLa cells in a dose-dependent manner (Fig. 5b), with

the half maximal inhibitory concentration (IC_{50}) about 5.78 μM upon irradiation. When the concentration of sample was evaluated to 20 μM, the surviving fractions of Hela cells were only 22.25 ± 4.75%, while the cell survival rate of A549 cells was as high as 75.25 ± 4.75%, further indicating the selectively accumulation of Por 4 in cancer cells high expression of folate receptors.[31] These results clearly confirmed that the synthesized Por 4 with active targeting group could be used as an efficient photosensitizer for cancer therapy.

Conclusions

In summary, we have synthesized and characterized a new photosensitizer (Por 4), where the methoxyporphyrin (Por 2) was conjugated with folic acid using ethylenediamine as a linker. Por 4 exhibited high efficiency of singlet oxygen generation because of the heavy atom effect. Moreover, due to the conjugation of folic acid, Por 4 could target specifically the cancer cells with overexpression of FR (HeLa cells) via FR-mediated endocytosis. Accordingly, Por 4 can selectively accumulate in HeLa cells, leading to a remarkable photodynamic therapeutic effect under irradiation. Thus, the synthesized Por 4 with good biocompatibility, remarkable photodynamic therapeutic effect and tumor-targeting properties, could be used as a potential photosensitizer for cancer with overexpresssion of folate receptor.

Experimental sections

Materials and Instruments

All chemicals were of reagent-grade, purchased from Sigma-Aldrich and used without further purification. All analytical-grade solvents were dried by standard procedures, distilled and deaerated before use. ^{1}H NMR spectra were recorded on a Varian Mercury-VX 300 spectrometer. The UV-vis spectra were carried out on a UV-vis Spectrophotometer (Shimadzu). The fluorescence spectra were performed on a PE LS55 fluorescence spectrometer. The chemical shifts were referenced to tetramethylsilane, TMS (d = 0.00). Mass spectra, reported as m/z, were obtained either on a Bruker Autoflex MALDI-TOF mass spectrometer or a Finnigan TSQ 710 (FAB-MS) mass spectrometer.

Synthesis of carboxyl acid porphyrin (Por 1)

Por 1 was synthesized according to the method reported in the literature with minor modification. [32] To a 250 mL three-neck flask, 3, 4, 5-trimethoxybenzaldehyde (2.94 g , 15 mmol), 4-formylbenzoic acid (0.76 g, 5 mmol) and 180 mL propionic acid were added. The resulting solution was then heated to reflux, followed by the addition of freshly distilled pyrrole (1.92 mL, 20 mmol) within 15 min. After refluxing for another 1 h, the solvent was evaporated in vacuo. The residue was dissolved in CH_2Cl_2 and extracted with saturated aqueous $NaHCO_3$ solution until the organic layer was neutral. The organic layer was then concentrated and the residue was purified by silica gel column chromatography (MeOH in CH_2Cl_2, 0-1% v/v) to get the desired product, yield 10%. ^{1}HNMR (400 MHz, $CDCl_3$): δ (ppm) = 8.99 (d, 8H), 8.40 (d, 4H), 7.49 (s, 6H), 3.98 (t, 27H), -2.79 (br s, 2H); MALDI-TOF MS: calcd for: 929.98, found: 929.28; UV-vis (DMF): λ= 422, 516, 552, 591, 648 nm.

Synthesis of platinum porphyrin complex (Por 2)

Por 1 (100 mg, 0.108 mmol) and potassium tetrachloroplatinate (89.7 mg, 0.215 mmol) were dissolved in 15 mL benzonitrile. The mixture was then heated to reflux for 48 h. The completion of metal insertion was verified by UV-vis spectroscopy and TLC. The solvent was evaporated in vacuo and the residue was subjected to silica column chromatography (MeOH in CH_2Cl_2: 0-2% v/v). The pure fraction was collected and concentrated to give the product 82 mg, yield 78%. ^{1}HNMR (400 MHz, $CDCl_3$): δ (ppm) = 8.83 (d, J = 7.8 Hz, 8H), 8.33 (d, J = 10.6 Hz, 4H), 7.40 (s, 6H), 3.82 (s, 27H); MALDI-TOF MS: calcd for: 1121.28, found: 1121.28; UV-vis (DMF): λ= 406, 511, 540 nm.

Synthesis of carboxyl-activated ester porphyrin (Por 3)

In the dark and under an inert atmosphere, Por 2 (30 mg, 0.027 mmol) was dissolved in a mixture of 8 mL pyridine and 0.2 mL dichlorosulfoxide, After stirring at 50 °C in the dark for 30 min, N-hydroxysuccinimide (180 mg, 0.06 mmol) was added and then stirred for another 3 h. The purification of the crude compound was performed using a silica gel column with CH_2Cl_2 as an eluent. After recrystallization in CH_2Cl_2/hexane solutions, the desired product was obtained in yield 73%. ^{1}HNMR (400 MHz, $CDCl_3$): δ (ppm) = 8.90 (d, J = 7.8 Hz, 6H), 8.68 (d, J = 4.9 Hz, 2H), 8.54 (d, J = 7.8 Hz, 2H), 8.32 (d, J = 8.0 Hz, 2H), 7.43 (s, 6H), 4.06 (s, 27H), 2.99 (s, 4H); MS (ESI): m/z =1219 $[M]^+$, 1026.9 $[M\text{-}Pt+2H]^+$. Anal. Calcd for $C_{58}H_{49}N_5O_{13}Pt$: C, 57.14; H, 4.05; N, 5.74. Found: C, 57.19; H, 4.02; N, 5.78.

View Article Online
DOI: 10.1039/C9OB00698B

Synthesis of ethyl folate (FA 3)

Folic acid (44.1 mg, 1.0 mmol) was activated with N,N'-dicyclohexylcarbodiimide (DCC) (24.8 mg, 1.2 mmol) and N-hydroxysuccinimide (NHS) (23 mg, 2.0 mmol) in 30 mL of dimethyl sulfoxide (DMSO) at 50 °C for 6 h, which was then reacted with ethylenediamine (60 mg, 10 mmol) with pyridine (15 μL) as a catalyst at room temperature. After 24 h, the precipitate formed was removed by filtration. 20 mL diethyl ether was added to the filtrate to obtain the yellow solid, which was then washed with 50 mL of acetone/diethyl ether solution (30:70% v/v ratio) and diethyl ether (3×50 mL) to remove traces of unreacted reagents and diisopropylethylammonium (NHS) salt. The product was dried in vacuum overnight and the yield was 60%. ^{1}HNMR (400 MHz, $CDCl_3$): δ (ppm) = 8.68 (s, 1H), 8.15-7.99 (m, 1H), 7.7-7.52 (m, 2H), 7.3-6.8 (m, 3H), 6.63-6.5 (m, 2H), 4.45 (br s, 2H), 4.26 (m, 1H), 3.32-3.19 (m, 4H), 3.1 (m, 2H), 2.15-1.79 (m, 4H). MS (ESI): *m/z* =483.73 $[M+H]^+$.

Synthesis of folic acid-platinum porphyrin conjugates (Por 4)

To a 50 mL two-neck flask, FA 3 (42.85 mg, 0.089 mmol), Por 3 (15 mg, 0.029 mmol), N,N-diisopropylethylamine (47 mg, 0.36 mmol) and DMF (0.7 mL) were added in the dark under a nitrogen atmosphere. After stirring at ambient temperature for 24 h, the mixture was gradually poured into a vigorously stirred solution of anhydrous Et_2O (20 mL).The dark brown precipitate obtained was collected by filtration, washed with Et_2O and CH_2Cl_2 and dried under vacuum to get 8.5 mg product, yield 34%. ^{1}H NMR (400 MHz, $CDCl_3$) δ 8.86 (s, 6H), 8.73-8.63 (m, 3H), 8.22 (s, 6H), 8.01 (s, 1H), 7.53 (d, *J* = 9.6 Hz, 2H), 7.37 (d, *J* = 14.2 Hz, 4H), 7.00 (s, 3H), 6.59 (s, 2H), 4.69 (s, 2H), 4.67-4.63 (m, 1H), 4.09 (dd, *J* = 8.7 Hz, 27H), 2.96 (s, 2H), 2.88 (s, 2H), 2.23 (d, J = 8.4 Hz, 4H). MS (ESI): *m/z* =1122.39 $\{M-[H_2CCH_2\text{-NH-FA}]\}^+$. Anal. Calcd for $C_{75}H_{69}N_{13}O_{15}Pt$: C, 56.74; H, 4.38; N, 11.47. Found: C, 56.29; H, 4.31; N, 11.17. UV-Vis (DMF): λ= 406, 511, 540 nm.

UV-vis absorption and fluorescence spectra

The UV-vis absorption spectrum and fluorescence spectrum of four porphyrin conjugates were measured in DMF solution. Fluorescence quantum yield (φ_f) of an unknown sample is calculated by using Eq. (1)[33].

View Article Online
DOI: 10.1039/C9OB00698B

$$\varphi_f = \varphi_f^R \frac{I_f}{I_f^R}\left(\frac{n}{n^R}\right)^2 \qquad (1)$$

Where, φ_f^R is the known fluorescence quantum yield of the reference sample (referred by the superscript 'R'); I_f and I_f^R are the integrated fluorescence intensities of the unknown sample and reference sample, respectively; A and A^R are the absorbance of the unknown sample and reference sample, respectively; n and n^R are the refractive indices of the solvents for the unknown sample and reference sample, respectively. The fluorescence quantum yield of the samples are measured at room temperature relative to that of TPP in THF solution ($\varphi_f^R = 0.052$)[33].

Singlet oxygen detection

The production of singlet oxygen was established qualitatively using 1,3-diphenylisobenzofuran (DPBF) as a singlet oxygen fluorescent probe. The absorbance change of DPBF at 418 nm could be assigned to the signal of consumption of singlet oxygen. During the experiment, the absorbance of the $^1O_2$ scavenger (DPBF) was adjusted to around 1.0 in air-saturated DMSO. The experiments were initially performed with about 45 μM DPBF. The photosensitizer was added and its concentration was adjusted to around 1 μM. After measurements were taken in the dark, the cuvette was exposed to LED lamp at the peak absorption wavelength for 10 seconds. The absorbance was measured several times after each irradiation. Each of the photosensitizers was irradiated 6 times. The singlet oxygen quantum yields of the synthesized porphyrins was calculated using Eq. (2) with 5,10,15,20-tetraphenylporphyrin (TPP) as the reference ($\phi_\Delta^R = 0.64$).

$$\phi_\Delta^S = \phi_\Delta^R \frac{k^S F^R}{k^R F^S} \qquad (2)$$

ϕ_Δ^R is the singlet oxygen quantum yield of the reference. Superscript S and R indicate the sample and reference compound respectively, k is the plot slop of the change in absorbance of DPBF (at 410 nm) with the irradiation time and F is the absorption correction factor, which is given by $F=1-10^{-OD}$. OD is the corresponding absorbance at irradiation wavelength.[34]

Cell viability assays

The potentiality of Por 4 as photosensitizer was tested using human cervical cancer cell line (HeLa cells) and human non-small cell lung cancer cell lines (A549 cells), where HeLa cells highly expressed folate receptors while lowly expression in A549 cells . The cytotoxic activity of the conjugate was evaluated using MTT assay. After treating the selected cell lines with Por 4 at different concentrations (0, 1, 2, 5, 10, and 20 μM in DMEM) for 24 h at 37 °C, MTT assay was performed to detect the surviving fraction of cells. HeLa cells and A549 cells were cultured in DMEM (Dulbecco Modified Eagle Medium) supplemented with 5% FCS (fetal calf serum), 100 U/mL penicillin, 100 μg/mL streptomycin at 37 ^{o}C and 6% CO_2. HeLa cells were first seeded in 96-well plates for 24 h and then treated with sample overnight in the dark. Cytotoxicity was determined by MTT reduction assay. The cell monolayer was washed twice with phosphate buffered saline (PBS) and then incubated with 50 μL of MTT solution (0.5 mg/mL) at 37 ^{o}C for 3 h. After removing the medium, 100 μL of DMSO was added. The solution was shaken for 30 min to dissolve the formed crystal in living cells. Absorbance was measured at a dual wavelength of 540 nm and 690 nm on a Labsystem Multiskan plate reader (Merck Eurolab, Switzerland). Each dosing concentration was performed in triplicate wells and repeated twice for MTT assay.

The photocytotoxicity of samples in HeLa cells and A549 cells was assessed by a similar protocol. Cells were first seeded in 96-well plates at 3× 10^3 cells per well for 24 h. The cells were then treated with sample in the dark overnight. Afterwards, the cell was exposure to yellow light (4 J/cm^2) produced from a 400 W tungsten lamp fitted with a heat-isolation filter and a 500 nm long-pass filter. The fluence rate was 6 mW/cm^2. Cell viability was determined by the MTT reduction assay.

FR-mediated targeting for HeLa cells

Laser scanning confocal microscope was applied to detect the FR-mediated targeting of the sample for cancer cells. For comparison, A549 cells with low expression of FR and HeLa cells with high expression of FR were selected for the biological studies, respectively.[35] Cancer cells were seeded on 3.5 cm well with cover slips and then cultured in the DMEM medium (10%) for two days. Afterward, cells were incubated with Por 4 at a concentration of 2.0 μM for 4 h at 37 °C and 5% CO_2. The cells were then washed three times with PBS solution before imaging on a confocal microscope.

Subcellular localization

HeLa cells were cultured in RPMI 1640 medium (Gibco^{Tm}) containing 10% fetal calf serum and 1% antibiotic penicillin and streptomycin (P/S), and cultured at 37 °C in a humidified 5% CO_2 atmosphere. Cells (6×10^3 cells per well) were seeded in 6-well plates (with sterile coverslips in each well) and incubated for two days at 37 °C in a humidified 5% CO_2 atmosphere. After renewal with the new medium, the cells were incubated with a photosensitizer at a concentration of 1.0 μM for 4 h at 37 °C. After that, the supernatant was carefully removed and the cells were washed three times with PBS. Subsequently, the slides were mounted and observed by a Zeiss Laser Scanning Confocal Microscope (LSM7 DUO), and then analyzed using ZEN 2009 software (Carl Zeiss).

Co-staining of porphyrin, LysoTracker Green and Hoechst 33342: HeLa cells were first incubated with porphyrin at 37 °C for 4 h and then further incubated with LysoTracker Green (50 nM) and Hoechst 33342 (50 nM) for 10 min at 37 °C. The cells were washed three times with PBS solution before imaging on a confocal microscope.

Acknowledgments

We are thankful for the support from National Natural Science Foundation of China (21601142), Natural Science Foundation of Hubei Province (2017CFB689), Zhejiang Provincial Natural Science Foundation of China (LY18B010002), and the 10th Graduate Innovative Fund of Wuhan Institute of Technology (CX2018023).

References

[1] Mari, C.; Pierroz, V.; Ferrari, S.; Gasser, G. Combination of Ru(II) complexes and light: new frontiers in cancer therapy. *Chem. Sci.*, **2015**, 6, 2660.

[2] Wu, F.; Yue, L.; Su, H.; Wang, K.; Yang, L.; Zhu, X. Carbon Dots @ Platinum Porphyrin Composite as Theranostic Nanoagent for Efficient Photodynamic Cancer Therapy. *Nanoscale. Res. Lett.,* 2018, 13, 357.

[3] Zhu, S.; Wu, F.; Wang, K.; Zheng, Y.; Li, Z.; Zhang, X.; Wong, W. Photocytotoxicity, cellular uptake and subcellular localization of amidinophenylporphyrins as potential photodynamic therapeutic agents: An in vitro cell study. *Bioorg. Med. Chem. Lett.,* **2015**, 25, 4513.

[4] Yao, S.; Zheng, Y.; Jiang, L.; Xie, C.; Wu, F.; Huang, C.; Wang, K. Methylene violet 3RAX-conjugated porphyrin for photodynamic therapy: synthesis, DNA photocleavage, and cell study. *RSC. Adv.*, **2018**, 8, 4472.

[5] Wu, F.; Chen, J.; Li, Z.; Su, H.; Leung, K. C.; Wang, H.; Zhu, X. Red/Near-Infrared Emissive Metalloporphyrin-Based Nanodots for Magnetic Resonance Imaging-Guided Photodynamic Therapy In Vivo. *Part. Part. Syst. Char.,* **2018**, 35, 1800208.

[6] Xu, Z.; Yu, F.; Wu, F.; Zhang, H.; Wang, K.; Zhang, X. Synthesis, DNA photocleavage, singlet oxygen photogeneration and two photon absorption properties of ruthenium-phenanthroline porphyrins. *J. Porphyr. Phthalocya.,* **2015**, 19, 1046.

[7] Zheng, Y.; Zhu, S.; Jiang, L.; Wu, F.; Huang, C.; Li, Z. Synthesis, singlet oxygen generation, photocytotoxicity and subcellular localization of azobisporphyrins as potentially photodynamic therapeutic agents in Vitro Cell Study. *J. Porphyr. Phthalocya.,* **2017**, 21, 122.

[8] Cheng, M.; Cui, Y.; Wang, J.; Zhang, J.; Zhu, L.; Kong, D. G-Quadruplex/Porphyrin Composite Photosensitizer: A Facile Way to Promote Absorption Redshift and Photodynamic Therapy Efficacy. *ACS Appl. Mater. Interfaces*., **2019**, 11, 13158.

[9] Wu, F.; Su, H.; Cai, Y.; Wong, W. K.; Jiang, W.; Zhu, X. Porphyrin-implanted Carbon Nanodots for Photoacoustic Imaging and in Vivo Breast Cancer Ablation. *ACS. Appl. Bio. Mater.,* **2018**, 1, 110.

[10] Srinivasan, M.; Rajabi, M.; Mousa, S. Multifunctional Nanomaterials and Their Applications in Drug Delivery and Cancer Therapy. *Nanomaterials.*, **2015**, 5, 1690.

[11] Morgat, C.; MacGrogan, G.; Brouste, V.; Velasco, V.; Sevenet, N.; Bonnefoi, H.; Fernandez, P.; Debled, M.; Hindie, E. Expression of Gastrin-Releasing Peptide Receptor in Breast Cancer and Its Association with Pathologic, Biologic, and Clinical Parameters: A Study of 1,432 Primary Tumors. *J. Nucl. Med.*, **2017**, 58, 1401.

[12] Vankayala, R.; Kuo, C. L.; Nuthalapati, K.; Chiang, C. S.; Hwang, K. C. Nucleus - Targeting Gold Nanoclusters for Simultaneous In Vivo Fluorescence Imaging, Gene Delivery, and NIR - Light Activated Photodynamic Therapy. *Adv. Funct. Mater.*, 2015, 25, 5934.

[13] Kuthala, N.; Vankayala, R.; Li, Y. N.; Chiang, C. S.; Hwang, K. C. Engineering Novel Targeted Boron-10-Enriched Theranostic Nanomedicine to Combat against Murine Brain Tumors via MR Imaging-Guided Boron Neutron Capture Therapy. *Adv. Mater.*, **2017**, 29, 1700850.

[14] Ho, L. C.; Wu, W. C.; Chang, C. Y.; Hsieh, H. H.; Lee, C. H.; Chang, H. T. Aptamer-Conjugated Polymeric Nanoparticles for the Detection of Cancer Cells through "Turn-On" Retro-Self-Quenched Fluorescence. *Anal. Chem.*, **2015**, 87, 4925.

[15] Farokhzad, O. C.; Cheng, J.; Teply, B. A.; Sherifi, I.; Jon, S.; Kantoff, P. W.; Richie, J. P.; Langer, R. Targeted nanoparticle-aptamer bioconjugates for cancer chemotherapy in vivo. *P. Natl. Acad. Sci. USA.*, **2006**, 103, 6315.

[16] Assaraf, Y. G.; Leamon, C. P.; Reddy, J. A. The folate receptor as a rational therapeutic target for personalized cancer treatment. *Drug. Resist. Updat.*, **2014**, 17, 89.

[17] Ledermann, J. A.; Canevari, S.; Thigpen, T. Targeting the folate receptor: diagnostic and therapeutic approaches to personalize cancer treatments, *Ann. Oncol.*, **2015**, 26, 2034.

[18] Zeng, L.; Luo, L.; Pan, Y.; Luo, S.; Lu, G.; Wu, A. In vivo targeted magnetic resonance imaging and visualized photodynamic therapy in deep-tissue cancers using folic acid-functionalized superparamagnetic-upconversion nanocomposites. *Nanoscale.*, **2015**, 7, 8946.

[19] Grossman, M.; Born, B.; Heyden, M.; Tworowski, D.; Fields, G. B.; Sagi, I.; Havenith, M. Correlated structural kinetics and retarded solvent dynamics at the metalloprotease active site, *Nat. Struct. Mol. Biol.*, **2011**, 18, 1102.

[20] Hilgenbrink, A. R.; Low, P. S. Folate receptor-mediated drug targeting: From therapeutics to diagnostics, *J. Pharm. Sci.*, **2005**, 94, 2135.

[21] Pinhassi, R. I.; Assaraf, Y. G.; Farber, S.; Stark, M.; Ickowicz, D.; Drori, S.; Domb, A. J.; Livney, Y. D. Arabinogalactan - Folic Acid - Drug Conjugate for Targeted Delivery and Target - Activated Release of Anticancer Drugs to Folate Receptor-Overexpressing Cells. *Biomacromolecules*., **2010**, 11, 294.

[22] Tan, Q. L.; Zhang, X. L.; Mao, L. J.; Xin, G. Q.; Zhang, S. F. Novel zinc porphyrin sensitizers for dye-sensitized solar cells: Synthesis and spectral, electrochemical, and photovoltaic properties. *Angew. Chem. Int. Ed.*, **2016**, 128, 5311.

[23] Yang, K.; Zhang, X.; Yang, F.; Wu, F.; Zhang, X.; Wang, K. DNA Photocleavage and Binding Modes of Methylene Violet 3RAX and its Derivatives: Effect of Functional Groups. *Aust. J. Chem.,* **2017**, 70, 830.

[24] Jiang, J.; Liu, D.; Zhao, Y.; Wu, F.; Yang, K.; Wang, K. Synthesis, DNA binding mode, singlet oxygen photogeneration and DNA photocleavage activity of ruthenium compounds with porphyrin-imidazo[4,5-f] phenanthroline conjugated ligand. *Appl. Organomet. Chem.,* **2018,** 32, e4468.

[25] Lincoln, R.; Kohler, L.; Monro, S.; Yin, H. M.; Stephenson, M.; Zong, R. F.; Chouai, A.; Dorsey, C.; Hennigar, R.;Thummel, R. P.; McFarland, S. A. Exploitation of Long-Lived 3IL

Excited States for Metal - Organic Photodynamic Therapy: Verification in a Metastatic Melanoma Model. *J. Am. Chem. Soc.*, **2013**, 135, 17161

[26] Zhu, S.; Yao, S.; Wu, F.; Jiang, L.; Wong, K.; Zhou, J.; Wang, K. Platinated porphyrin as a new organelle and nucleus dual-targeted photosensitizer for photodynamic therapy. *Org. Biomol. Chem.,* **2017**, 15, 5764.

[27] Yang, M.; Deng, J.; Guo, D.; Sun, Q.; Wang, Z.; Wang, K.; Wu, F. Mitochondria-targeting Pt/Mn porphyrins as efficient photosensitizers for magnetic resonance imaging and photodynamic therapy. *Dyes Pigments.*, **2019**, *166*, 189-195.

[28] Wu, F.; Yang, M.; Zhang, J.; Zhu, S.; Shi, M.; Wang, K. Metalloporphyrin-indomethacin conjugates as new photosensitizers for photodynamic therapy. *J. Biol. Inorg. Chem***., 2019,** 24, 53.

[29] Banfi, S.; Caruso, E.; Caprioli, S.; Mazzagatti, L.; Montia, E. Photodynamic effects of porphyrin and chlorin photosensitizers in human colon adenocarcinoma cells. *Bioorg. Med. Chem.*, **2004**, 12, 4853.

[30] Chizhova, N. V.; Kulikova, O. M.; Mamardashvili, N. Zh. Synthesis and Properties of ms - and β-Substituted Pt(II) and Pt(IV) Tetraphenylporphyrinates. *Russ. J. Gen. Chem.*, **2013**, 11, 2108.

[31] Liu, P. Stabilization of layer-by-layer engineered multilayered hollow microspheres. *Adv. Colloid. Interfac.*, **2014**, 207, 178.

[32] Lee, C. W.; Lu, H. P.; Lan, C. M. Novel Zinc Porphyrin Sensitizers for Dye-Sensitized Solar Cells: Synthesis and Spectral, Electrochemical, and Photovoltaic Properties. *Chem Eur. J.*, **2009**, 15, 1403.

[33] Ghosh, M.; Mora, A. K.; Nath, S.; Chandra, A. K.; Hajra, A.; Sinha, S. Photophysics of soret-excited free base tetraphenylporphyrin and its zinc analog in solution. *Spectrochim. Acta. A.,* **2013**, 116, 466.

[34] Meng, S.; Xu, Z.; Hong, G.; Zhao, L.; Zhao, Z.; Guo, J.; Ji, H.; Liu, T. Synthesis, Characterization and In Vitro Photodynamic Antimicrobial Activity of Basic Amino Acid-Porphyrin Conjugates. *Eur. J. Med. Chem.*, **2015**, 92, 35.

[35] Canal, F.; Vicent, M. J.; Pasut, G.; Schiavon, O.; Control, J. Relevance of folic acid/polymer ratio in targeted PEG-epirubicin conjugates. *J. Control. Release.*, 2010, 146, 388.